Pergamon

PII: S0042-6989(97)00068-0

Vision Res., Vol. 37, No. 22, pp. 3097–3107, 1997

Printed in Great Britain
0042-6989/97 $17.00 + 0.00

Scaling Effects in the Perception of Higher-order Spatial Correlations

JULIAN S. JOSEPH,*‡ JONATHAN D. VICTOR,† LANCE M. OPTICAN*

Received 27 March 1996; in revised form 6 December 1996; in final form 18 March 1997

Human texture discrimination depends both on spatial-frequency content and on higher-order or multi-point correlations. Spatial-frequency discrimination exhibits a high degree of scale invariance over a range of several octaves, but the scaling behavior of sensitivity to higher-order correlation structure is unknown. We explored the scale dependence of texture discrimination for image ensembles which shared the same power spectrum, but differed in their higher-order correlations. Literally scaling the ensembles so that they occupy larger retinal regions results in discrimination performance that is largely independent of scale over a 3 octave range. Holding the display size constant and scaling the texture being sampled within the display over the same range produces performance that varies with scale appreciably. The ideal observer performance is computed, and the absolute efficiency is seen to be quite small, on the order of 10^{-2}–10^{-1}. As the texture is scaled down, increasing the number of checks within the fixed display size, performance increases while the efficiency decreases. These dependencies remain when the stimulus onset asynchrony is increased from 50 to 500 msec. We created sets of textures which varied both in check number and correlation strength, for which ideal observer performance was equated. For the human observers, efficiency was significantly higher for textures with higher correlation strength, but fewer checks. These results are consistent with a model in which a fixed number of checks is processed in a scale-invariant manner, while the remainder of the display is processed much less efficiently. © 1997 Elsevier Science Ltd

Texture discrimination Higher-order correlations Scale invariance Absolute efficiency

INTRODUCTION

Changes in the scale of a visual stimulus are a natural source of variation in the retinal image that the human visual system must cope with in order to identify a surface or object. Under natural viewing conditions, scale changes occur due to variations in viewing distance. These scale changes are coupled to other visual cues such as stereoscopic disparity and occlusion, but it is unclear to what extent these cues are critical to distance-invariant object recognition. In order to isolate the effects of scale changes alone, we sought to determine the effects of scale changes on the perception of a class of artificial grayscale visual textures (image ensembles), for which correlation structure could be manipulated independently of other size cues, including spatial-frequency content.

As the distance between the viewer and an object changes, so does the overall spatial-frequency content; for a sinusoidal grating target, spatial-frequency is proportional to distance. In a landmark study of spatial-frequency discrimination, Campbell *et al.* (1970) found a remarkably small variation of the Weber fraction as the reference frequency was varied across 4 octaves (see also Hirsch & Hylton, 1982). Variation of the reference frequency is equivalent to scaling the sinusoidal gratings that are to be discriminated, but displaying them through a window of fixed size.

For image recognition by human observers, spatial-frequency information is not as important as spatial phase information (Oppenheim & Lim, 1981; Piotrowski & Campbell, 1982). This may be partly because many of the features that allow observers to distinguish between images, such as edges and T-junctions, depend on the relative phases of the Fourier components. Therefore, aside from the perception of the amount of power in various spatial-frequencies, we would also like to know about the perception of higher-order aspects of form that contain phase structure.

A closely related problem to that of image discrimination is that of discrimination between image ensembles, i.e., collections or probability distributions of images (Julesz, 1962, 1980; Julesz *et al.*, 1978; Bergen & Julesz, 1983). This is a family of problems that the visual system

*Laboratory of Sensorimotor Research, National Eye Institute, NIH, Bethesda, MD 20892, U.S.A.

†Department of Neurology and Neuroscience, Cornell University Medical College, New York, NY 10021, U.S.A.

‡To whom all correspondence should be addressed at present address: Department of Psychology/296, University of Nevada, Reno, NV 89557, U.S.A. [*Tel* (702) 784-1129; *Fax* (702) 784-1126; *Email* jsj@unr.edu].

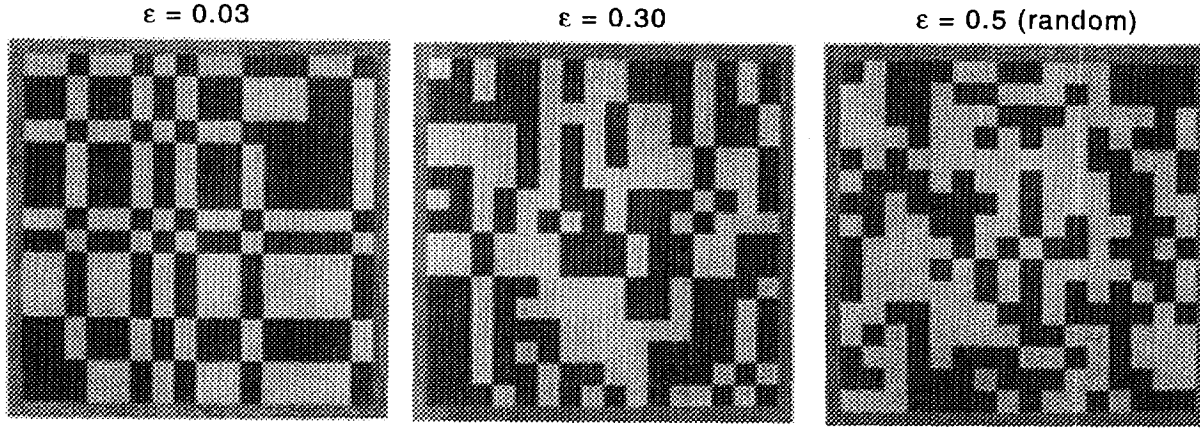

FIGURE 1. Sample images from the even texture with various degrees of propagated decorrelation. As the decorrelation parameter ε increases from 0 toward 0.5, the texture becomes increasingly decorrelated and unstructured.

must contend with whenever there is a need to ask "What kind of stuff am I looking at?" (Victor & Conte, 1989, 1991, 1993; Chubb & Landy, 1990, 1991; Bergen, 1991; Yellott, 1993; Victor, 1994; Chubb *et al.*, 1994). That is the question we are addressing by approaching the problem of form perception from the standpoint of image ensembles, referred to here as "textures", and the various types of structure they contain. Here, as well, the phase structure is important (Victor & Conte, 1996). The power spectrum of an ensemble is the ensemble average of the power spectra of the individual images comprising the ensemble; this contains the same information as the two-point ensemble correlations, and carries no phase information. The phase information is manifest in the higher-order or multi-point correlations, the correlations of the image luminance among three or more points over the ensemble. The higher-order correlations can be varied without changing the power spectrum, and for some kinds of higher-order correlations such differences alone are rapidly discriminable (Julesz *et al.*, 1978; Victor & Conte, 1991). The scale dependence of this type of image ensemble discrimination based solely on higher-order correlations is not known, and is the subject of this study.

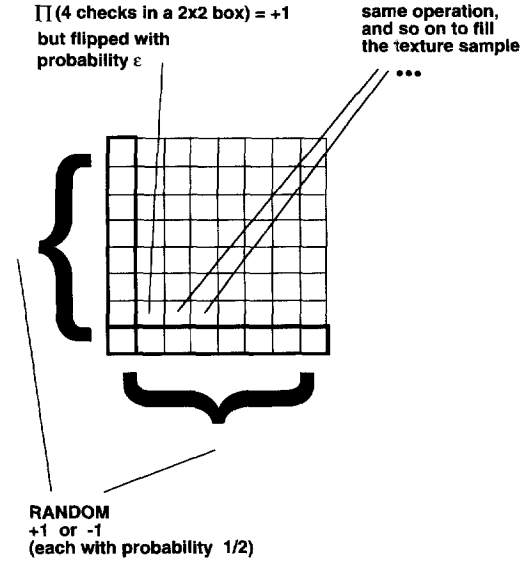

FIGURE 2. Construction of images drawn from the image ensemble that is the even texture with propagated decorrelation ε (see text).

GENERAL METHODS

Figure 1 shows images sampled from the textures (image ensembles) used in this study. The even texture with any given level of propagated decorrelation has a power spectrum which is white, like the completely random texture sampled at the far right of Fig. 1 (Victor & Conte, 1991). However, unlike the random texture, the even texture possesses spatial correlations of fourth-order and higher (the third-order correlations are zero). This means that the luminance values of four different points in the image have a correlation among them, in the ensemble sense. More specifically for even textures, there are correlations among any four points that form the corners of a rectangle. The construction of images sampled from the even texture with an amount of propagated decorrelation labeled ε is illustrated in Fig. 2. Each check is either bright or dark, with equal deviation from the background luminance level, and is referred to as either +1 or −1. The checks in the first row and first column are each chosen to be +1 or −1 with 50–50 probability. Starting in the second row, one sets the next check value so that the product of the checks in a 2×2 box equals +1. Then, with probability ε the check is flipped to the opposite sign. For the next check in the second row the same procedure is performed, and so on until the texture is filled. The procedure for generating these textures is not translation-invariant (the first row and column appear to be playing special roles), but the resulting texture has translation-invariant statistics. For $\varepsilon = 0$, one obtains the purely even texture with higher-order correlations among arbitrarily distant points. For $\varepsilon = 0.5$, one obtains the random texture, in which each check's luminance is chosen independently with a 50–50

probability. For values of the decorrelation ε in between these extremes, the correlations fall off exponentially with distance. Each texture in this class has the same power spectrum as the random texture, but it also possesses higher-order spatial correlations. Any two of these textures constitute an isodipole texture pair, which is a pair of textures (image ensembles) sharing the same mean luminance (first-order or one-point correlation) and power spectrum (second-order or two-point correlations). The two textures in such a pair differ, however, in their higher-order statistics.

In these experiments, we will measure human performance for discrimination between textures that are generated by this procedure. In all cases, one of the discriminand textures was a random texture ($\varepsilon = 0.5$), and the other was an *even* texture with checks of the same size and with a value of the "propagated decorrelation" ε between 0 and 0.5. As ε approaches 0, the texture becomes progressively more like the highly structured even texture (and thus, easier to discriminate from the random texture).

Stimuli were presented on a 60 Hz noninterlaced NEC 3DS monitor, with 800×600 resolution and approximately 32.5 pixels/cm, controlled by a Number Nine GXi TIGA card in a PC. Stimuli were viewed binocularly from a distance of 57 cm. The background and mean luminance in all displays were 75 cd/m^2. The contrast was 0.4.

A separate session was devoted to measurement of the discrimination performance for each texture pair considered. In each session, performance was stabilized by running five blocks of 100 trials, each with feedback. In the first of these blocks, the images were viewed freely rather than presented briefly. After 400 trials with 50 msec presentation, data were collected from two blocks without feedback. Each datum thus comprises 200 trials. In each block, there were 50 image samples from each discriminand ensemble. Sessions of different texture scale, display size, and decorrelation level were performed in random order.

Each trial was initiated by the subject by pressing a mouse button. As illustrated in Fig. 3, a 250 msec central fixation cross appeared, followed by a 250 msec blank interval. An image randomly chosen from one of the two discriminand ensembles was then presented for 50 msec. This was immediately followed by a 200 msec random white-noise mask of 95% contrast consisting of 2.3 min checks covering the texture display area.

Two naïve subjects and one author (JSJ) participated. All had normal or corrected-to-normal vision.

EXPERIMENT 1: LITERAL SCALING

We first consider the effects of literally scaling the texture pair involved in the discrimination, so that the retinal area being stimulated changes along with the scale of the texture (see Fig. 4). The number of checks in the textures that were presented were 8×8 and 16×16, with a display size in the range of 0.6–4.8 deg for the former, 1.2–4.8 deg for the latter.

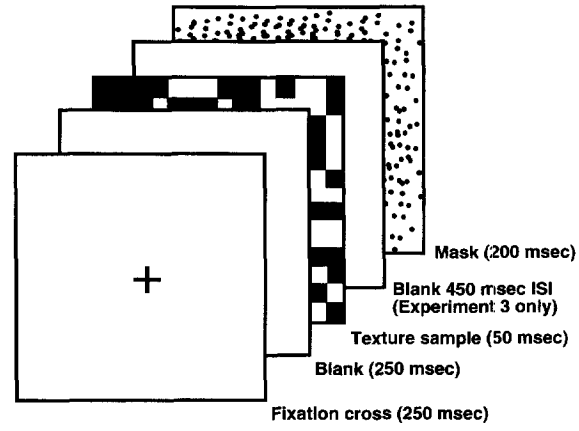

FIGURE 3. Stimulus sequence in each trial.

Results

The results are plotted in Fig. 5, showing d' as a function of check size for the 8×8 and 16×16 texture displays. For the 8×8 displays, scaling the texture by 3 octaves produced no statistically significant changes in performance level in any of the subjects. For the 16×16 displays, performance variation over 2 octaves of scale showed individual differences, but was generally weak. Subject TPR showed no significant difference in the performance over this range, while the ratio of d's across this range was 1.5 ± 0.3 and 0.6 ± 0.1 for AAA and JSJ, respectively. (Error bars here and in the figures represent 1 SEM.) In summary, we observed scale invariance for the 8×8 displays, and did not observe a consistent or strong scale dependence for 16×16 displays.

These results indicate that the mechanisms responsible for texture discrimination based on higher-order spatial correlations are robust with respect to changes in texture scale. This is nontrivial, considering that as the texture is scaled-up (increasing display size), new portions of the visual field are participating in the display, suggesting that detectors responsive to those regions are recruited for the discrimination. At the same time, the shift in the carrier frequency (1/check size) presumably requires the involvement of different detectors at the different scales because of the different spatial-frequency channels that are conveying the signal.

EXPERIMENT 2: SCALING WITH CONSTANT DISPLAY SIZE

Methods

In the previous experiment, different eccentricities participate in the display as the texture is scaled. To explore the effects of constraining the eccentricity in the presentation of textures of various scales, we held the display size constant in this experiment while scaling the textures (Fig. 6). We used a display size of 4.8 deg, which is the size of the largest displays in Experiment 1 (the 8×8 display of 36 min checks and the 16×16 display of

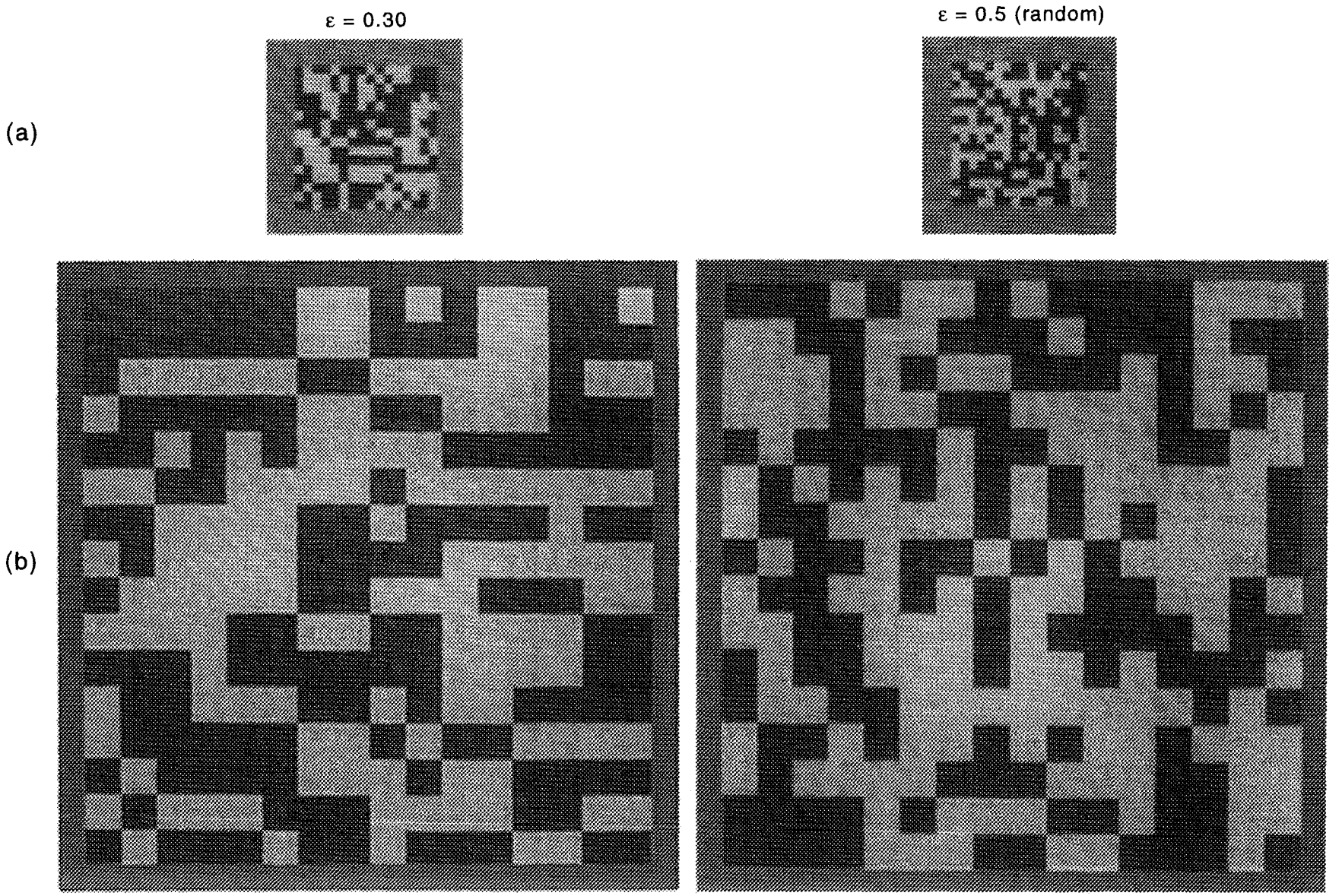

FIGURE 4. Experiment 1: Literal scaling. The two textures sampled in (a) serve as the discriminands for one ensemble discrimination, the texture pair in (b) for another. The two texture pairs are related by scaling.

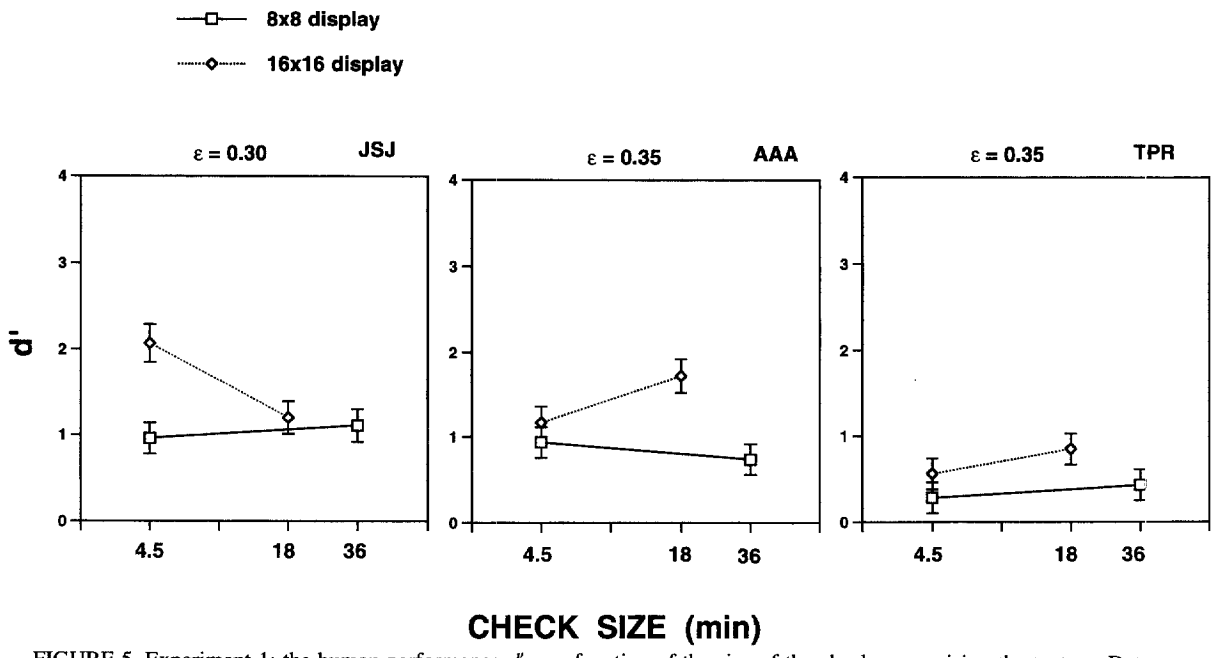

FIGURE 5. Experiment 1: the human performance d' as a function of the size of the checks comprising the texture. Data are shown for 8×8 and 16×16 texture displays for each of three subjects. Here, as in all the figures, the error bars represent 1 SEM.

18 min checks). All other aspects of the experiment are as described in General Methods above.

Results

The results are plotted in Fig. 7, using the same height for the d' axis as in Fig. 5 to facilitate comparison. There is a consistent decrease in performance as the check size is increased over 3 octaves. Each of the subjects showed this decrease ($P < 0.05$). This should be contrasted with the absence of changes in performance that we saw in Experiment 1, as 8×8 textures were scaled across the same 3-octave range. Therefore, the scale dependence we have observed with fixed display size cannot be due to the change in check size *per se*. Instead, it must be due to the decreased number of checks, or samples, as the check size is increased under the constraint of fixed display size.

Decreasing the number of checks in the images sampled from the texture naturally leads to decreasing ideal observer performance in the texture discrimination task. The ideal observer uses a Bayesian strategy, deciding which of the two textures being discriminated is more likely to have produced a given image. The ideal observer needs to estimate statistics from a finite sample; if the sample is small, there is a non-negligible chance of deciding that an image drawn from the random texture had, in fact, come from the structured texture, and vice verse. Figure 8 shows the performance of the ideal observer (d'_{IDEAL}), computed from the exact expression given in the Appendix. The horizontal axis of this plot corresponds with the check size that was plotted in Fig. 7. In the parameter range of interest, d'_{IDEAL} falls with the number of checks (N) as $N^{1/2}$ to an excellent approximation. Combined with the measured human performance of Fig. 7, we obtain the absolute efficiency, defined as $A = d'^2/d'^2_{\mathrm{IDEAL}}$. This is plotted in Fig. 9 as a function of check size. We find that the absolute efficiencies are quite small, usually in the order of 1–10%. We also find a consistent increase in the efficiency with check size, as we decrease the number of checks in the display.

EXPERIMENT 3: EFFECTS OF STIMULUS ONSET ASYNCHRONY (SOA)

Methods

It is conceivable that the decreased efficiency observed in Experiment 2 for larger numbers of checks may be entirely due to processing time limitations, if not all the spatial regions are processed in parallel. This experiment determines whether the scaling effects observed in Experiment 2 persist when the SOA is increased from 50 to 500 msec, maintaining the stimulus duration at 50 msec. A 450 msec blank interval is introduced after the presentation of the texture sample. Aside from this, the experiment was the same as Experiment 2.

Results

Figure 10 shows the task performance for both the 500 and the 50 msec SOA (replotted from Fig. 7). All subjects showed performance that was a decreasing function of check size over the 3-octave range tested. Extending the SOA 10-fold did not eliminate the scale dependence at fixed display size. All subjects showed improved performance for the longer SOA, at least for the 4.5 min checks; subjects AAA and JSJ showed such an increase for the 18 min checks as well. The absolute efficiency is shown in Fig. 11. Even with a 10-fold increase in SOA, absolute efficiency remains an increasing function of check size (and hence, a decreasing function of check number).

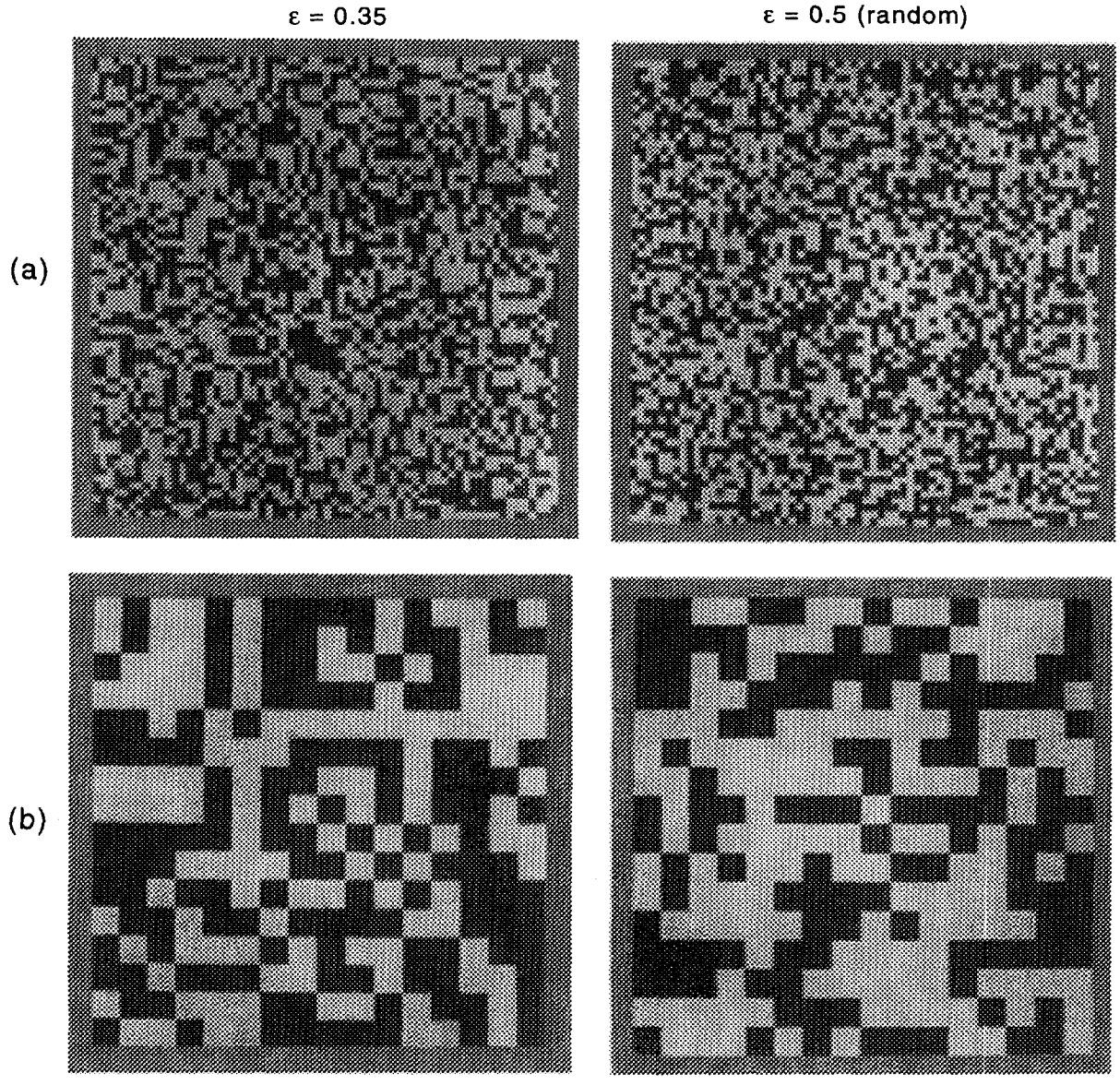

FIGURE 6. Stimuli for Experiments 2 and 3: scaling at fixed display size. The texture pair sampled in (a) is to be discriminated, and in a separate measurement the pair in (b) is discriminated. They are related by scaling, but sampled with a fixed display size.

EXPERIMENT 4: MATCHED IDEAL OBSERVER PERFORMANCE

Methods

At fixed display size, there are two qualitatively distinct parameters that govern the performance level, the number of checks and the amount of decorrelation. We would like to know which of these is more useful to the visual system. A natural means of carrying out such a comparison is to match the ideal observer performance between two discrimination tasks. One of the tasks has a larger number of checks (64×64 vs 16×16) but more decorrelation ($\varepsilon = 0.35$ vs $\varepsilon = 0.03$). Images drawn from these two texture pairs are shown in Fig. 12, which alone gives a convincing demonstration that the greater correlation strength, as opposed to increased sampling, allows human observers to distinguish textures more readily.

Results

Figure 13 shows the results, plotted as the percent correct obtained in each of the two tasks which are matched for d'_{IDEAL}. There is consistently improved performance when greater spatial coherence (smaller decorrelation ε) is present at the expense of having fewer checks in the display. Performance in this condition was near ceiling, so we plotted percent correct rather than d'. These results imply that the spatial correlations of higher-order are used more effectively by the visual system than further sampling of the texture by the addition of more checks into the image.

DISCUSSION

Results summary

To summarize, we have seen a large degree of scale

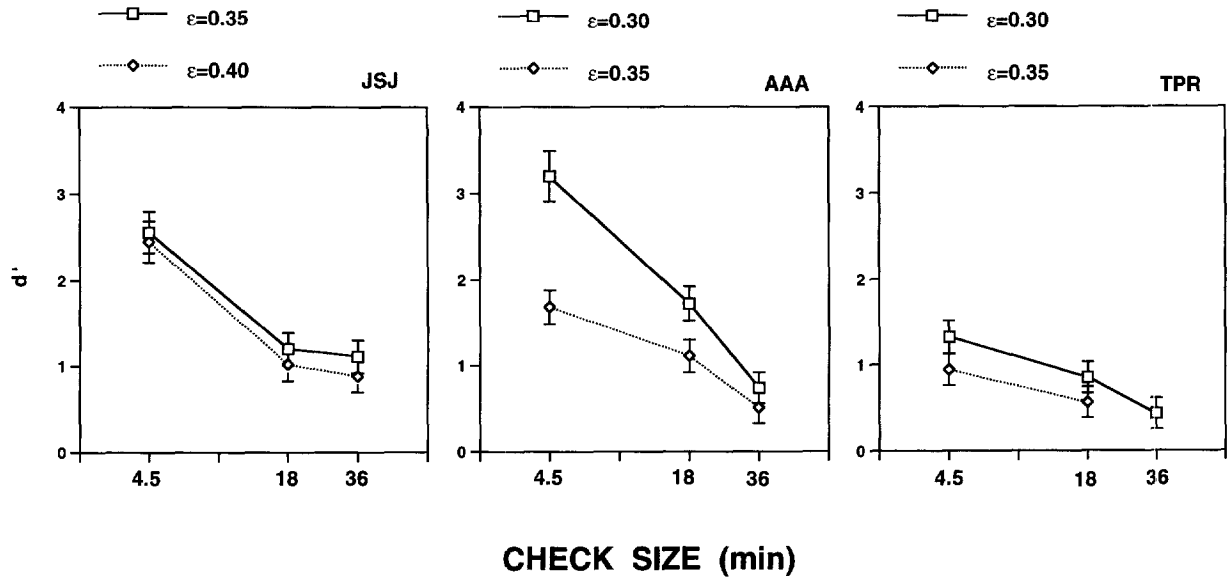

FIGURE 7. Experiment 2: performance d' as a function of check size. Because the display size is held constant, increasing checks size corresponds to decreasing number of checks. The 4.5 min checks appear in 64×64 displays, the 18 min checks in 16×16 displays, and the 36 min checks in 8×8 displays. Data are shown for two different values of the decorrelation for each subject.

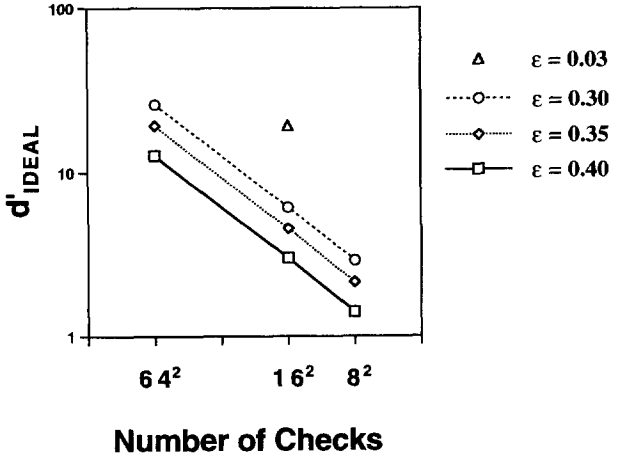

FIGURE 8. The ideal observer performance for discriminating an even texture with propagated decorrelation from a purely random texture, as a function of the number of checks in the texture and for various levels of the decorrelation. The points in the plot and those used throughout the paper were computed from the exact expression given in the Appendix. In the parameter regime of these experiments, d'_{IDEAL} is proportional to $N^{1/2}$ to an excellent approximation, where N is the number of checks.

invariance in the perception of higher-order or multi-point spatial correlations over 3 octaves in scale. The absolute efficiency of the processing of such correlations and any features that result from their presence is quite low. The values observed were typically on the order of 10^{-2}–10^{-1}. By contrast, holding the display size, and thus the retinal eccentricities, constant while the textures are scaled produces a scale dependence in the human performance. The performance increases with increasing number of checks in the texture samples, which for constant display size corresponds to decreasing texture scale. The ideal observer performance is also a decreasing function of scale in such circumstances, and decreases more rapidly than the human performance. Thus, the absolute efficiency increases with the texture scale; in other words, it is a decreasing function of the number of checks in the image. This scale dependence remains if the SOA is increased from 50 to 500 msec. This increase in the processing time results in a larger performance increase for the scales with larger numbers of checks. Keeping the ideal observer performance constant as well as the display size, while trading off the number of checks against the strength of the spatial correlations, reveals that the visual system makes more effective use of stronger correlations than it does greater numbers of checks that could potentially be sampled.

Implications for visual mechanisms

We now consider the ability of various models to account for these observations. Because the performance showed weak scale dependence in Experiment 1, in which the textures were literally scaled (display size not constant), we conclude that differences in spatial-frequency content *per se* cannot account for the scale dependence seen in Experiments 2 and 3, in which the display size was held fixed.

At least three distinct types of models for these results may be considered. In the first, all the checks are processed with the same efficiency, regardless of scale. This predicts the scale-invariance we observe with the literal scaling (Experiment 1), but fails to account for the change in efficiency with check number (Experiment 2). We therefore reject this type of model. In the second type of model, a fixed retinal area is admitted for processing,

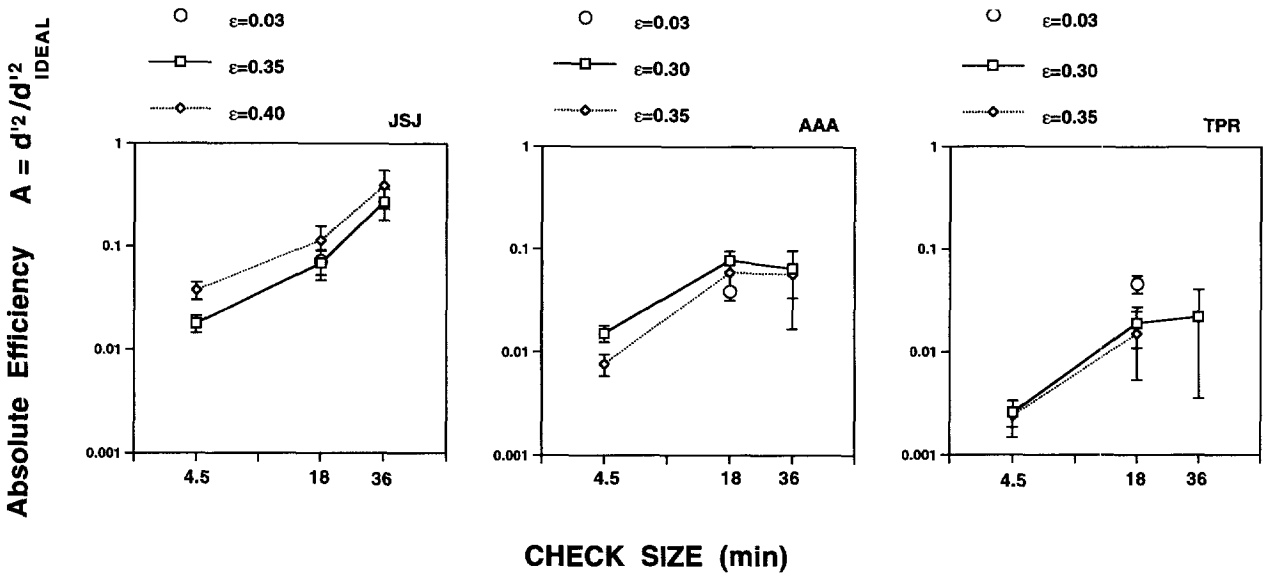

FIGURE 9. Experiment 2: absolute efficiency as a function of check size for constant display size.

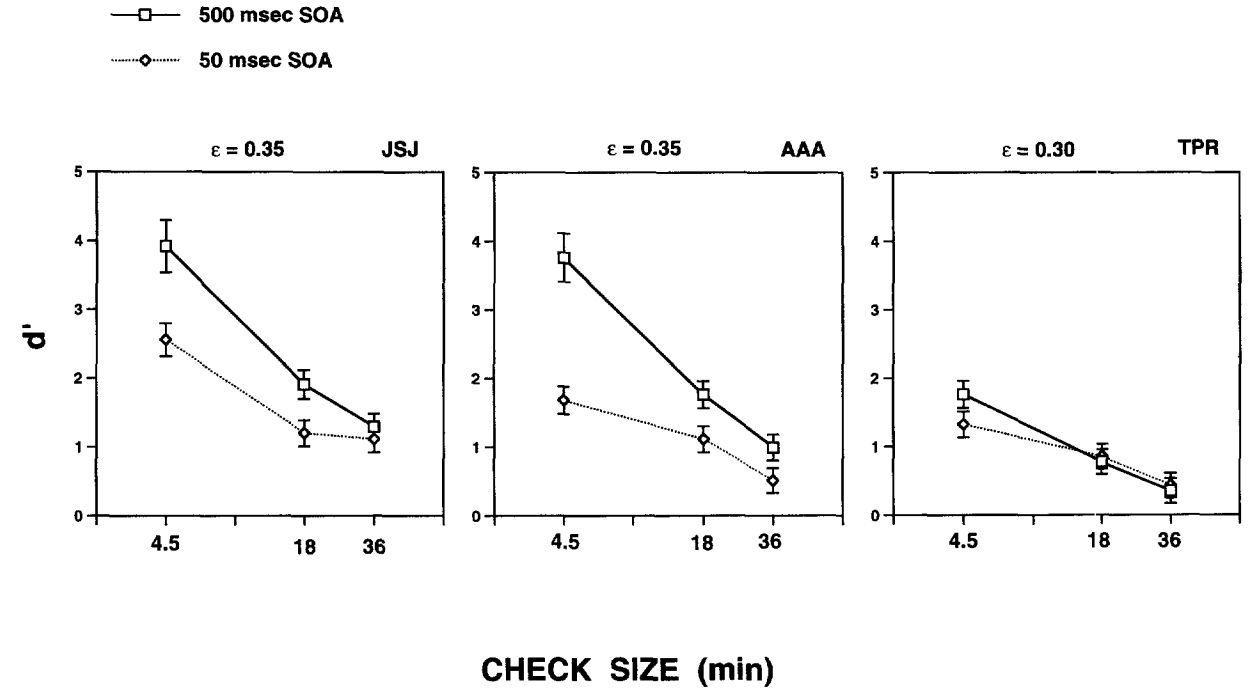

FIGURE 10. Experiment 3: effects of SOA. Performance as a function of check size for SOAs of 500 and 50 msec. Display size was held constant.

with all the checks falling within that area processed with the same efficiency. This model predicts a performance decrease with increasing check size in Experiment 1, and a flat efficiency in Experiment 2. Neither of these predictions are consistent with the data, and we reject this class of models.

In the third type of model, a fixed number of checks (regardless of scale) is processed all with the same efficiency. Assuming that this number is smaller than the smallest number of checks present in any of our images (64), this model predicts performance with flat scale dependence in Experiments 1 and 2. The former is qualitatively consistent with the data, but not the latter. This discrepancy can be eliminated, however, by augmenting the model with a second component: the inefficient processing of the remainder of the image, which may be considered as "background". The increased performance seen in Fig. 7 at the smaller check sizes (larger check numbers) can be the result of a very inefficient process acting on all the checks except the relatively few that are processed with an efficiency of one order of magnitude higher. Because there is such a large number of checks in the background in these cases, an appreciable change in performance may result.

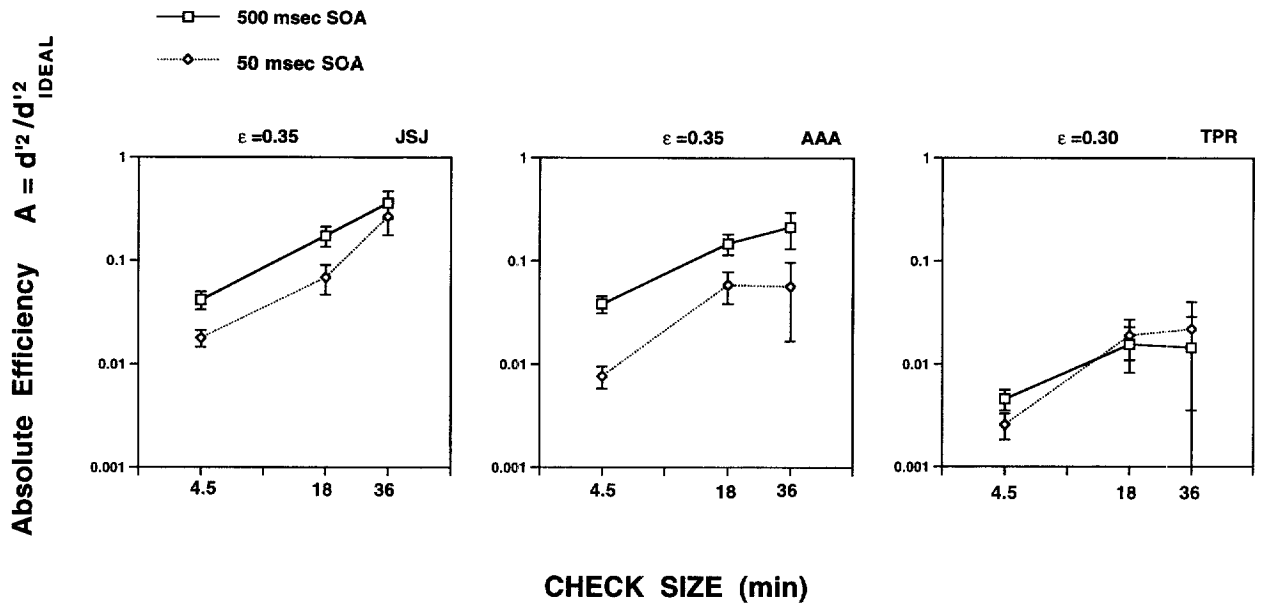

FIGURE 11. Experiment 3: efficiency for SOAs of 500 and 50 msec as a function of check size at fixed display size.

Within such a model framework, we can obtain a crude estimate of the number of checks that are being processed (apart from the background). Background contamination is least for the 8×8 displays (36 min check size). If we assume the checks that undergo privileged processing are processed ideally, we can compute a lower bound on the number of such checks from the data in Fig. 7 at the 36 min check size. The ideal performance based on an available number of checks N_{HUMAN} is a known function $d'_{IDEAL}(\varepsilon, N_{HUMAN})$ (see the Appendix). Equating this with the measured d' then gives N_{HUMAN}, the number of checks accepted for processing in this model. Across the three subjects this takes values in the range 4–20. Of course, the processing is less than ideal, and so these values place a lower bound on the number of checks that receive the bulk of the processing. Attention may play a role in selecting the relatively small fraction of checks that are the main beneficiaries of processing resources.

The results of Experiment 3 showed that the performance for 8×8 displays does not increase with SOA. This indicates that processing time is not a bottleneck for the small number of checks that are processed with a relatively high efficiency compared with the background (regardless of how ideally they are processed). By contrast, the observed performance increase with SOA for the 64×64 displays indicates that the less efficient background processing does not saturate quickly, i.e., within 50 msec.

We observed in Experiment 4 that, with the ideal observer performance matched, performance was significantly better for textures containing stronger correlations at the expense of having fewer checks. In the light of the model we have suggested, this could be interpreted as follows. The (small) number of checks admitted to processing is the same for the two texture pairs. The ideal observer performance based on these checks alone is greater when the correlations are stronger. Greater human performance is then to be expected. The inefficient processing of the remaining background checks is not strong enough to reverse the much stronger effect of the mismatch in the signal carried by the chiefly processed checks.

Possible physiologic mechanisms

The scale invariance we have identified is consistent with the results of the VEP analysis of Victor & Conte (1989), who found a length scale for nonlinear cortical processing of higher-order correlations which was proportional to check size over a wide range. While the neural mechanisms for such computations are at present unknown, we note that neurons in V1 do respond differentially to the correlation structure we have studied (Purpura *et al.*, 1994), and that these responses are present across a wide range of scales.

Relation to other scaling studies

Scale invariance has been observed in human form perception in a variety of other contexts. Nothdurft (1985) investigated texture segregation based on line orientation as a function of both line spacing and line length. He observed that performance degraded with increased spacing when the line length was kept constant but not when it was scaled proportionately. In this case, the two textures being segregated have different power spectra. Parish & Sperling (1991) found that identification of bandpass-filtered letters with added gaussian noise is scale-invariant, depending not on retinal spatial-frequency but on object spatial-frequency. Toet *et al.* (1987) observed that spatial displacement thresholds for gaussian blobs scale proportionately as the separation between the blobs and their width are scaled together.

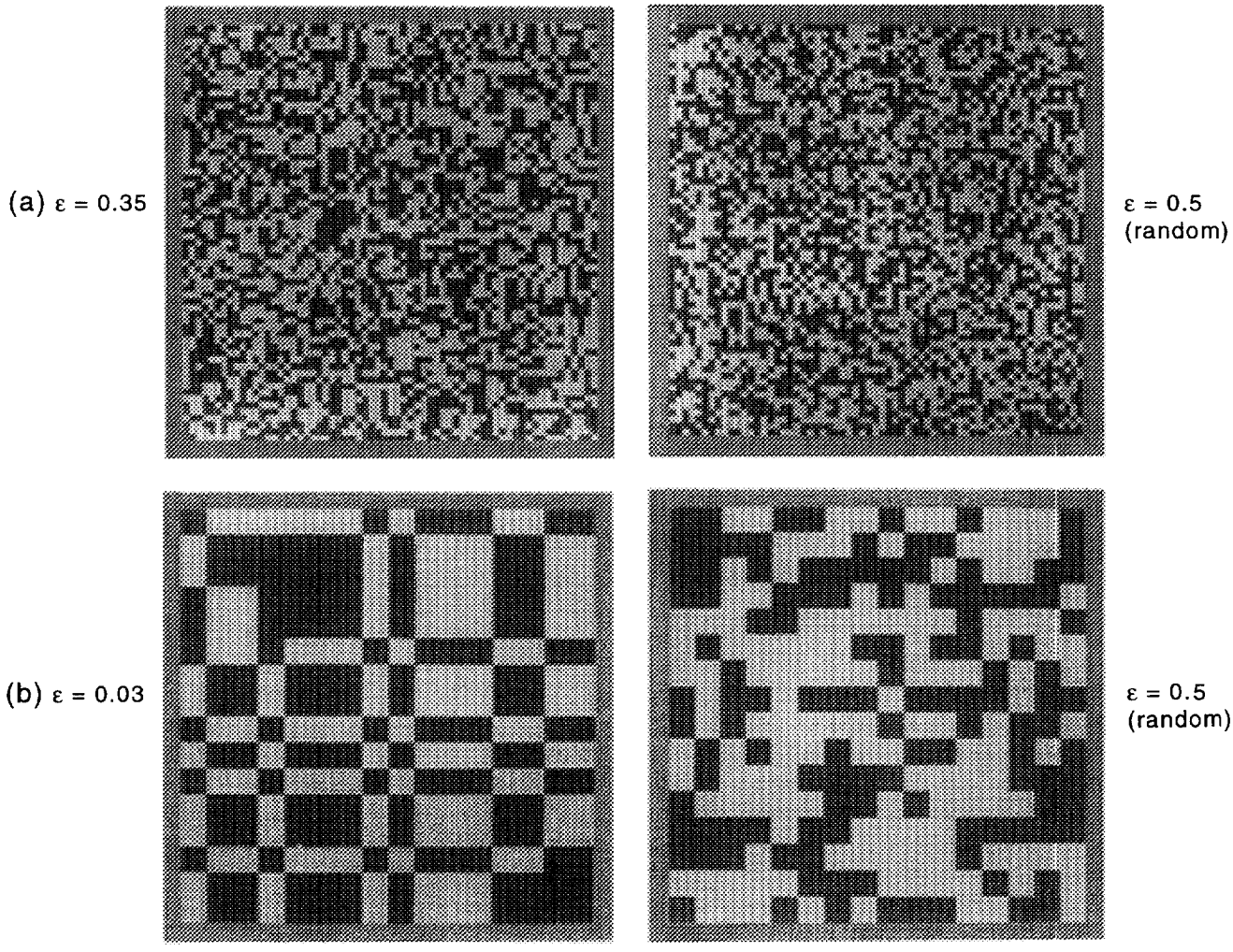

FIGURE 12. Experiment 4: matched ideal observer performance. Samples from the two texture pairs tested that share a common value of d'_{IDEAL}. The structured ensemble in pair (a) has more checks than the one in pair (b), but has weaker correlations.

Levi *et al.* (1990) found that thresholds in the bisection of intervals between blurred lines scale in proportion with the line separation and blur width over a wide range. These few examples illustrate the diversity of the perceptual phenomena exhibiting scale invariance, which now includes the perception of multi-point or higher-order spatial correlations.

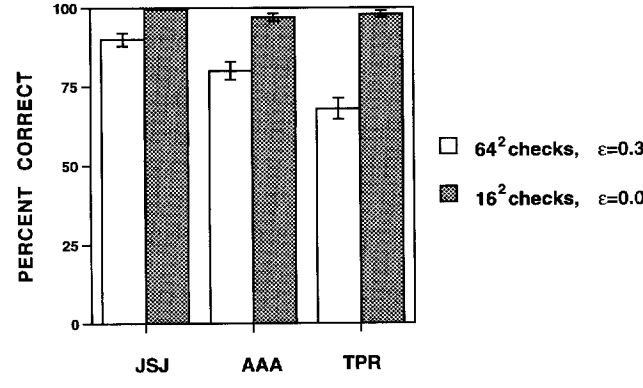

FIGURE 13. Results of Experiment 4: matched ideal observer performance. Percent correct is shown for each texture pair. Stronger correlations are more useful for performance than having more checks sampling the texture.

REFERENCES

Bergen, J. R. (1991). Theories of visual texture perception. In Regan, D. (Ed.), *Vision and Visual Dysfunction*, Vol. 10. Boston, MA: CRC Press.

Bergen, J. R. & Julesz, B. (1983). Rapid discrimination of visual patterns. *IEEE Transactions on Systems, Man, and Cybernetics, SMC-13*, 857–863.

Campbell, F. W., Nachmias, J. & Jukes, J. (1970). Spatial-frequency

discrimination in human vision. *Journal of the Optical Society of America, 60*, 555–559.
Chubb, C. & Landy, M. S. (1990). Orthogonal distribution analysis: a systematic approach to the study of texture perception. *Investigative Ophthalmology and Visual Science, 31*, 561(suppl.).
Chubb, C. & Landy, M. S. (1991). Orthogonal distribution analysis: a new approach to the study of texture perception. In Landy, M. S. & Movshon, J. A. (Eds), *Computational models of visual processing*. Cambridge, MA: MIT Press.
Chubb, C., Econopouly, J. & Landy, M. S. (1994). Histogram contrast analysis and the visual segregation of IID textures. *Journal of the Optical Society of America A, 11*, 2350–2374.
Hirsch, J. & Hylton, R. (1982). Limits of spatial-frequency discrimination as evidence of neural interpolation. *Journal of the Optical Society of America, 72*, 1367–1374.
Julesz, B. (1962). Visual pattern discrimination. *I.R.E. Transactions on Information Theory, IT-8*, 84–92.
Julesz, B. (1980). Spatial nonlinearities in the instantaneous perception of textures with identical power spectra. *Philosophical Transactions of the Royal Society of London B, 290*, 83–94.
Julesz, B., Gilbert, E. N. & Victor, J. D. (1978). Visual discrimination of textures with identical third-order statistics. *Biological Cybernetics, 31*, 137–140.
Levi, D. M., Jiang, B.-C. & Klein, S. A. (1990). Spatial interval discrimination with blurred lines: black and white are separate but not equal at multiple spatial scales. *Vision Research, 30*, 1735–1750.
Nothdurft, H. C. (1985). Sensitivity for structure gradient in texture discrimination tasks. *Vision Research, 25*, 1957–1968.
Oppenheim, A. V. & Lim, J. S. (1981). The importance of phase in signals. *Proceedings of the IEEE, 69*, 529–541.
Parish, D. H. & Sperling, G. (1991). Object spatial frequencies, retinal spatial frequencies, noise, and the efficiency of letter discrimination. *Vision Research, 31*, 1399–1415.
Piotrowski, L. N. & Campbell, F. W. (1982). A demonstration of the visual importance and flexibility of spatial-frequency amplitude and phase. *Perception, 11*, 337–346.
Purpura, K. P., Victor, J. D. & Katz, E. (1994). Striate cortex extracts higher-order spatial correlations from visual textures. *Proceedings of the National Academy of Sciences USA, 91*, 8482–8486.
Toet, A., van Eekhout, M. P., Simons, H. L. J. J. & Koenderink, J. J. (1987). Scale invariant features of differential spatial displacement discrimination. *Vision Research, 27*, 441–451.
Victor, J. D. (1994). Images, statistics, and textures: implications of triple correlation uniqueness for texture statistics and the Julesz conjecture: comment. *Journal of the Optical Society of America A, 11*, 1680–1684.
Victor, J. D. & Conte, M. M. (1989). Cortical interactions in texture processing: scale and dynamics. *Visual Neuroscience, 2*, 297–313.
Victor, J. D. & Conte, M. M. (1991). Spatial organization of nonlinear interactions in form perception. *Vision Research, 31*, 1457–1488.
Victor, J. D. & Conte, M. M. (1993). Lack of global power spectral contributions to isodipole discrimination, as assessed by manipulations of spatial phase. *Investigative Ophthalmology and Visual Science, 34*, 1238(suppl.).
Victor, J. D. & Conte, M. M. (1996). The role of high-order phase correlations in texture processing. *Vision Research, 36*, 1615–1631.
Yellott, J. I. (1993). Implications of triple correlation uniqueness for texture statistics and the Julesz conjecture. *Journal of the Optical Society of America A, 10*, 777–793.

Acknowledgements—J.S.J. is grateful to K. Nakayama for his hospitality during the writing of this manuscript, the National Eye Institute for fellowship F32-EY06531, and K. Purpura for helpful conversations. J.D.V. was supported by National Eye Institute EY7977.

APPENDIX

The ideal observer performance for discriminating between the random texture and an even texture with propagated decorrelation ε can be expressed in a form that lends itself to computation readily. The ideal observer can, in principle, walk through a given image and count exactly how many checks were flipped by the decorrelation process when the image was generated. Because each check in the image is generated in the same way (apart from the first row and column), it is only the total number of flipped checks in the image that enters into the decision of which ensemble the image belongs to. This quantity is binomially distributed. The optimal strategy is to say "random" if, and only if, the number of flips is greater than or equal to some critical number n_c. The fraction correct obtained by the ideal observer is:

$$P_c = \frac{1}{2}\sum_{k=0}^{n_c-1}(1-\varepsilon)^{M-k}\varepsilon^k\binom{M}{k} + \left(\frac{1}{2}\right)^{M+1}\sum_{k=n_c}^{M}\binom{M}{k}$$

where N = the number of checks = m^2 for an $m \times m$ display, $M = (m-1)^2$ and n_c = the smallest integer larger than $M\ln[1/(2(1-\varepsilon))]/\ln[\varepsilon/(1-\varepsilon)]$. (That this is the critical value of n_c can be seen from the fact that the change in performance upon decrementing n_c becomes negative below this critical value. This value therefore maximizes P_c. This is the finite difference analog of the value at which P_c has zero derivative and is thereby maximized.) The first term represents the correct classification of images from the structured ensemble. The second term corresponds to correct classification from the random ensemble. The points plotted in Fig. 8 and the ideal observer performance values used in calculating absolute efficiencies throughout this paper are computed from this exact expression. The d'_{IDEAL} is calculated from the above fraction correct P_c by the relation:

$$P_c = (2\pi)^{-1/2}\int_{-\infty}^{d'/2} dx\, e^{-\frac{1}{2}x^2}$$

In the parameter range of these experiments, the d'_{IDEAL} that one computes from this expression is proportional to $N^{1/2}$ to an excellent approximation. This can be shown using standard analytical approximations: replacing the sum by an integral, approximating the binomial by a gaussian, extending the integration limits to infinity, and using the asymptotic expansion for the error function.